Total inelastic pion multiplicity distribution in 250-GeV/c $\pi^- p$ interactions

R. N. Diamond,* P. J. Hays,† S. Hagopian, and J. E. Lannutti
Florida State University, Tallahassee, Florida 32306
(Received 6 December 1982)

Semi-inclusive π^0 multiplicity distributions for 2—14 charged prongs are obtained using a generating-function approach based on an expansion in terms of Mueller moments. The four-prong data require the explicit assumption of a two-component model. Under this assumption and the further assumption of no three-neutral-particle correlations, the total pion multiplicity is obtained. The total multiplicity shows peaking at even prongs, indicative of G-parity-conserving diffractive processes which dominate at lower multiplicities. The cross section for these processes is ~ 4 mb.

I. INTRODUCTION

One of the first quantities reported by bubble-chamber experiments is the multiplicity distribution of the recorded events. These distributions for the most part pertain only to the charged-particle multiplicities.[1] Some information on neutral-particle production, such as the mean number $f_1^{\pi^0}$ and two-particle correlations $f_2^{\pi^0}$, has been presented but, because of limited statistics, the semi-inclusive neutral and hence the total pion multiplicity distributions have not been reported. A number of models have appeared in the literature[2] which purport to describe the multiplicity distributions of the produced particles. Many of these models make similar predictions for charged-particle production, but differ on their neutral-particle predictions. In order to distinguish between many of these models and to further test the notion that two components[3,4] are needed to describe particle production, the neutral multiplicity distributions provide valuable new information.

II. EXPERIMENTAL DETAILS

The experiment (E-234) was carried out in the Fermilab 15-ft bubble chamber filled with liquid hydrogen, and involved a 46 000-picture exposure to a 250-GeV/c π^- beam. A kicker magnet in the beam line was used to limit the flux to an average of four beam tracks per exposure. The large fiducial volume gave the chamber a high detection efficiency for neutral strange particles and for γ rays which result primarily from π^0 decay. We have previously published results on strange particles[5] and inclusive π^0 production based on a measured subsample of the film.[6]

The results presented here are based primarily on the scan information, although certain parameters such as the momentum-dependent γ-ray-conversion probability are based on the measurements. In all that follows we neglect the presence of charged strange particles, treating them as pions also. The scan results are summarized in Tables I—III. From Table I we see that of the 40 337 frames deemed usable for doing γ-ray physics, 8567 were rejected because they had more than 15 beam tracks. The neutral secondaries were put into one of three categories by the scanners: G for secondaries with essentially 0° opening angles and with at least one track showing the characteristic spiraling of an electron, V for secondaries with nonzero opening angles or with heavily ionizing or interacting tracks, and A for secondaries with $\sim 0°$ opening angles which were ambiguous between G and V. Subsequent measurements and kinematic fitting of the A secondaries revealed that $\sim 90\%$ were actually γ-ray conversions. Table II shows the GA multiplicities from the scan for

TABLE I. Scan results.

Category	First scan	Rescan	Conflict scan
Total frames	40 337	6 659	5 957
Good frames	31 770	5 035	4 444
Bad frames	8 567	1 624	1 513
No. of beam tracks	109 884	19 669	17 575
No. of events	22 330	3 904	3 656
No. of G's	12 565	2 180	2 139
No. of A's	12 545	2 234	2 319
No. of V's	2 505	402	440
No. of GA's	25 110	4 414	4 458
Events with $GA=0$	9 617	1 635	1 441
Events with $GA=1$	5 936	1 071	1 003
Events with $GA=2$	6 777	1 198	1 212

TABLE II. Distribution of *GA*'s for corrected primary charged-particle multiplicity. The elastic two-prong events have been removed.

Prongs	*GA*'s 0	1	2	3	4	5	6	7	8	9	⟨*GA*⟩	Total events
0	14	3	4	0	0	0	0	0	0	0	0.53	21
2	641	439	202	79	30	8	2	0	0	0	0.90	1402
4	1796	837	401	178	76	28	8	3	1	0	0.81	3328
6	1615	1161	662	282	132	48	20	10	1	1	1.10	3931
8	1462	1225	750	390	175	74	40	5	3	2	1.28	4127
10	1013	1037	693	348	159	74	34	7	4	2	1.42	3371
12	674	648	467	271	141	60	25	11	4	0	1.53	2310
14	355	411	304	175	98	47	21	5	4	2	1.67	1422
16	192	226	145	117	51	22	13	4	4	1	1.71	774
18	80	124	75	47	31	17	7	2	1	1	1.82	386
20	36	42	48	29	14	9	4	3	1	0	2.04	185
22	14	23	14	10	8	3	5	1	0	0	2.09	78
24	9	10	7	7	5	5	1	1	1	0	2.38	47
26	1	1	4	0	1	0	1	0	0	0	2.48	8
28	1	1	1	1	1	0	1	0	0	0	3.09	5
30	0	0	0	0	0	0	1	0	0	0	6.00	1
Total events	7903	6198	3775	1932	921	395	183	52	25	10	1.26	21 395

each charged multiplicity. An average of 1.26 *G* or *A* secondaries was found for each event.

Table I indicates that three scans took place. Approximately 15% of the film was rescanned for purposes of obtaining the scanning efficiency. 90% of the rescanned frames were subject to a conflict scan in order to resolve any differences between the first two scans.

The charged-particle multiplicity distribution shown in Table II has been corrected for a number of effects including (1) unresolved secondary interactions, (2) unobserved recoil protons, (3) hidden *G* or *A* vertices near the primary vertex, (4) hidden *V*'s, (5) Dalitz pairs, (6) hidden neutral strong interactions, and (7) missed two-prong events. The details of these corrections can be found in Ref. 4.

The scanning efficiencies for this film are presented in Table III. The two-prong events clearly have a lower scan efficiency ("finding" efficiency ϵ_f) than other topologies. However, if neutral secondary vertices such as γ-ray conversions are visible, the two-prong events have a better chance of being noted. This situation has another consequence, namely that the two-prong sample, being relatively enriched with respect to *GA* vertices because of the lower scan efficiency for two-prong events without *GA*'s, has a greater potential length and therefore a higher conversion probability for the γ rays. The identification efficiency ϵ_I has several components, primarily the probability ($\sim$95%) that a *GA* is actually a γ ray and the probability ($\sim$72%) that the γ ray is associated with the primary vertex, i.e., gives a three-constraint kinematic fit.

III. RESULTS

A. Method of parametrizing the data

The charged-particle multiplicity distribution is easily obtained from the scan information once the corrections

TABLE III. Scan efficiencies. The identification efficiency is the probability that a *GA* is in reality a γ-ray conversion associated with the primary vertex.

	Prongs	0 *GA*	1 *GA*	2 *GA*	> 3 *GA*
Primary vertices					
Finding efficiency	2	0.69±0.02	0.85±0.04	0.74±0.08	0.72±0.12
	12	0.91±0.03	0.91±0.03	0.99±0.01	0.97±0.01
	All others	0.919±0.005	0.919±0.005	0.919±0.005	0.919±0.005
GA's					
Finding efficiency	2		0.76±0.05	0.67±0.07	0.90±0.05
	All others		0.767±0.005	0.767±0.005	0.767±0.005
Identification efficiency	2		0.48±0.05	0.48±0.05	0.48±0.05
	4		0.58±0.05	0.58±0.05	0.58±0.05
	≥6		0.63±0.02	0.63±0.02	0.63±0.05
Conversion efficiency	2		0.160±0.004	0.160±0.004	0.160±0.004
	≥4		0.139±0.003	0.139±0.003	0.139±0.003

mentioned in Sec. II are determined. The neutral pion multiplicity distributions, however, must be inferred from the observed *GA* distributions. Because of the relatively low detection efficiency, the π^0 distribution at high multiplicity is largely determined by events with high numbers of *GA* vertices, a statistically meager sample. We therefore restrict ourselves to events with 2–14 charged prongs where the *GA* sample is usable.

We use a generating-function technique applied to moments analyses[7,8] to evaluate the π^0 multiplicity distribution. This technique is described in the Appendix.

To compute the π^0 moments (and σ_n's) we visualize the production of *GA*'s as shown in Fig. 1. The first step is the production of π^0's according to an as-yet-unknown multiplicity distribution. Let $\Phi_{\pi^0}(g)$ be the frequency-generating function (FGF) for the π^0's and $\Phi_\gamma(h_\gamma)$ be the FGF for the γ's coming from the 2γ decay of the π^0's. The argument h_γ is the generator for γ's. These FGF's are related by

$$\Phi_\gamma(h_\gamma)=\Phi_{\pi^0}(h_\gamma{}^2) . \tag{1}$$

Conceptually we regard the γ's as "decaying" into γ's which convert with probability ϵ_c in the bubble chamber, γ_c, or into γ's which do not convert and are consequently lost, γ_l. We can substitute

$$h_\gamma=\epsilon_c\gamma_c+(1-\epsilon_c)\gamma_l . \tag{2}$$

In a similar fashion we consider the converted γ's, γ_c, as decaying into γ's which are either found by the scanners, γ_f, or else missed by them, γ_m. If the probability of a scanner finding a converted γ ray is ϵ_f, we can set

$$\gamma_c=\epsilon_f\gamma_f+(1-\epsilon_f)\gamma_m . \tag{3}$$

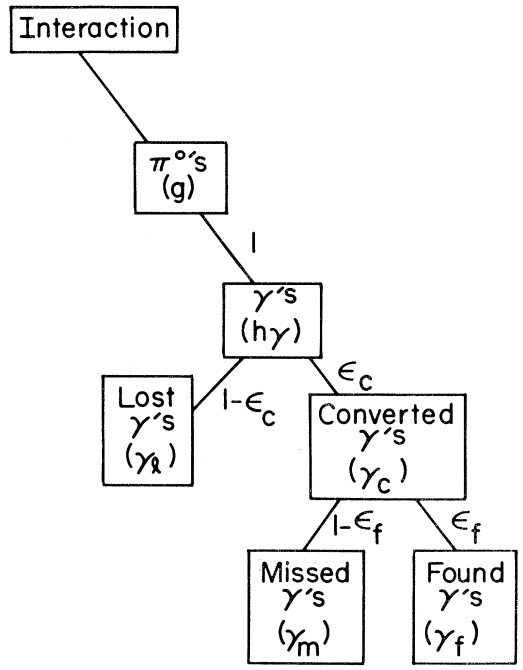

FIG. 1. Decay chain used in generating-function approach to π^0 multiplicity distribution.

In Eqs. (2) and (3) γ_c, γ_l, γ_f, and γ_m are, respectively, the generators for γ's converted, lost, found, or missed. The FGF for γ's which convert in the bubble chamber and are found by the scanners is obtained by substituting Eqs. (2) and (3) into Eq. (1) to give

$$\Phi_\gamma(\gamma_f)=\Phi_{\pi^0}([\epsilon_c\epsilon_f\gamma_f+\epsilon_c(1-\epsilon_f)\gamma_m+(1-\epsilon_c)\gamma_l]^2) . \tag{4}$$

γ's which failed to convert or were not found are neglected by setting $\gamma_m=\gamma_l=1$ in Eq. (4). Then

$$\Phi_\gamma(\gamma_f)=\Phi_{\pi^0}((\epsilon_c\epsilon_f\gamma_f+1-\epsilon_c\epsilon_f)^2) . \tag{5}$$

We are actually interested in the FGF for *GA*'s and given the generator g for *GA*'s we have

$$\Phi_{GA}(g\epsilon_I+1-\epsilon_I)=\Phi_\gamma(g) , \tag{6}$$

where ϵ_I is the probability that a *GA* is indeed a γ ray associated with the primary event. Using Eqs. (5) and (6) we have

$$\Phi_{GA}(g)=\Phi_{\pi^0}([(\epsilon_c\epsilon_f/\epsilon_I)g+1-(\epsilon_c\epsilon_f/\epsilon_I)]^2) \tag{7}$$

or equivalently

$$\Phi_{\pi^0}(r)=\Phi_{GA}(w\sqrt{r}+1-w) , \tag{8}$$

where $w=\epsilon_I/\epsilon_c\epsilon_f$. The second Mueller moment[9] for the *GA*'s is obtained from the *GA*'s FGF (see Appendix) by

$$f_2^{GA}=(\partial/\partial r)^2[\ln\Phi_{GA}(r+1)]_{r=0} . \tag{9}$$

By taking the appropriate derivatives of Eq. (8) we obtain

$$f_2^{\pi^0}=(w^2/4)f_2^{GA}-(w/4)f_1^{GA} . \tag{10}$$

Equation (10) relates the desired moment $f_2^{\pi^0}$ to the measured moment f_2^{GA}.

If a single-π^0 production mechanism is present, and if three-particle and higher-order correlations are small, then $f_n^{\pi^0}$ can be neglected for $n\geq 3$. From a knowledge of $f_1^{\pi^0}$ and $f_2^{\pi^0}$ we can derive the π^0 multiplicity using Eq. (A2) in the Appendix and the *GA* moments computed from Table II. The weights w in Eq. (8) are obtained from Table III. If two production mechanisms, say, diffractive and nondiffractive, are present the first two Mueller moments become

$$f_1^{\pi^0}=\alpha f_{1D}^{\pi^0}+(1-\alpha)f_{1N}^{\pi^0} , \tag{11}$$

$$f_2^{\pi^0}=\alpha f_{2D}^{\pi^0}+(1-\alpha)f_{2N}^{\pi^0}+\alpha(1-\alpha)(f_{1D}^{\pi^0}-f_{1N}^{\pi^0})^2 , \tag{12}$$

where the subscripts D and N refer to diffractive and nondiffractive components and α represents the relative amount of the diffractive component. The presence of two production mechanisms, even though each mechanism has f_n vanishing for $n\geq 3$, will lead to nonvanishing f_n if one assumes only a single production mechanism.

B. π^0 multiplicity distributions

The inclusive π^0 multiplicity distribution obtained from this moments analysis is shown in Fig. 2. The Mueller moments for the distribution are $f_1^{\pi^0}=3.52\pm0.39$, $f_2^{\pi^0}=3.3\pm1.0$, and $f_3^{\pi^0}=3.5\pm2.0$. Also plotted in Fig. 2

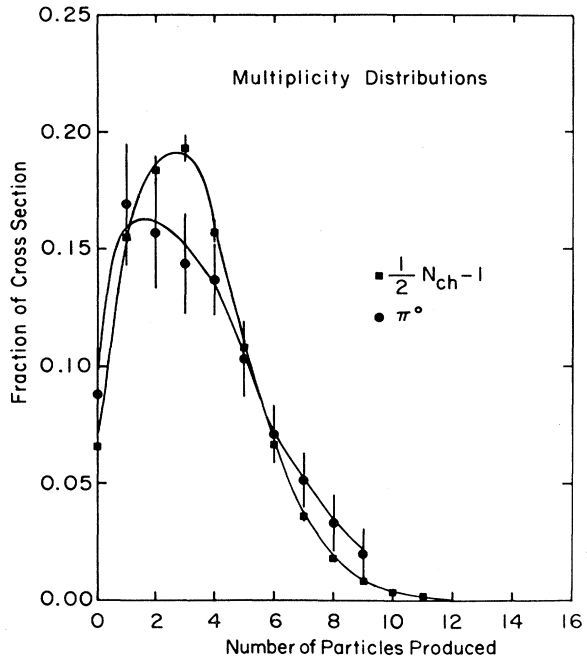

FIG. 2. Normalized inclusive π^0 and produced-charged-particle multiplicity distributions. The curves serve only to guide the eye.

is $\frac{1}{2}N_{ch}-1$ which represents the number n_p of produced π^- or π^+. The mean value of n_p is 3.17 ± 0.02 and the full width at half maximum (FWHM) is 4.86 ± 0.05 compared to 3.52 ± 0.39 and 6.1 ± 1.0, respectively, for the π^0's. We see that within errors the two distributions are consistent with each other. From this we can conclude that the production of π^0's is statistically the same as the production of charged π's. A nonzero $f_3^{\pi^0}$ is attributed to the presence of two components in the production process.

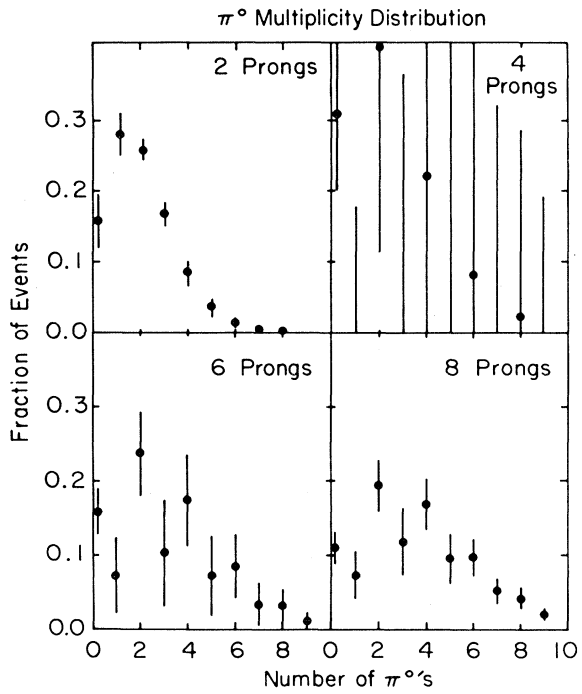

FIG. 3. Normalized π^0 multiplicity distribution for 2, 4, 6, or 8 charged prongs.

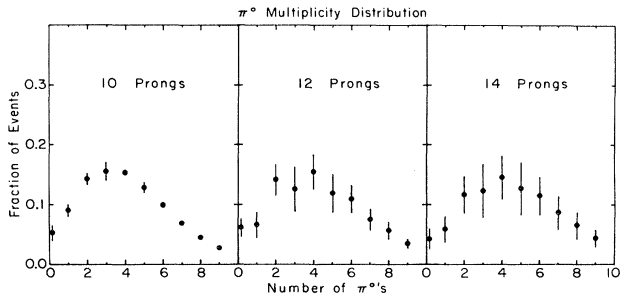

FIG. 4. Normalized π^0 multiplicity distribution for 10, 12, or 14 charged prongs.

A similar type of analysis has been carried out in order to obtain the semi-inclusive π^0 multiplicity distributions. For each charged multiplicity we assume that a single production process is dominant and that for each component we can take $f_n^{\pi^0}$ to be zero for $n \geq 3$. As evidenced by Figs. 3 and 4 these assumptions lead to reasonable-looking π^0 distributions for all charge multiplicities except for four prongs.

We believe that two components, a low-multiplicity diffractive component and a higher-multiplicity nondiffractive component, contribute about equally to the four prongs, but that the two prongs are dominated by the diffractive component and that the six- and higher-charged-prong events are dominated by the nondiffractive component. This notion is supported by Figs. 5 and 6 where

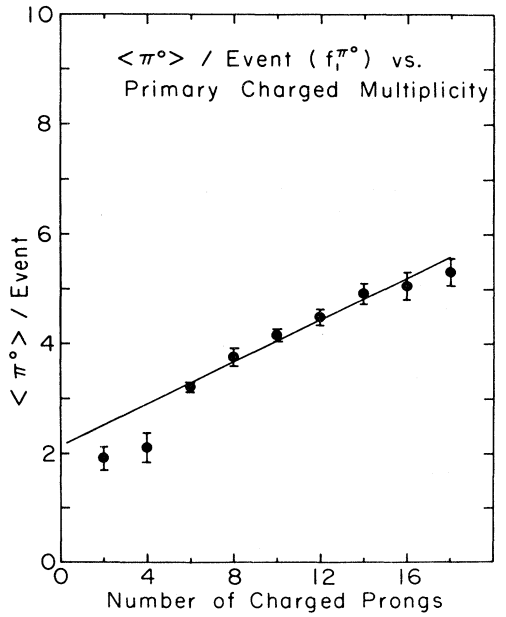

FIG. 5. The mean number of π^0's, $f_1^{\pi^0}$, plotted as a function of the primary charged multiplicity. The curve is a linear fit using 6—18 prongs.

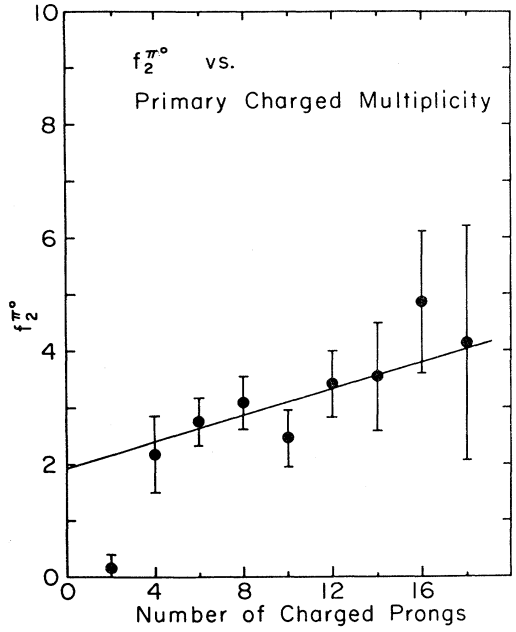

FIG. 6. The second Mueller moment $f_2^{\pi^0}$ plotted as a function of the primary charged multiplicity. The curve is a linear fit using 6—18 prongs.

we plot $f_1^{\pi^0}$ and $f_2^{\pi^0}$ as functions of the charged multiplicity. Linear fits to these data over the range of 6—18 prongs give

$$f_1^{\pi^0}(N_{\rm ch})=AN_{\rm ch}+B \tag{13}$$

with

$$A=0.191\pm0.015 \text{ and } B=2.14\pm0.15$$

and

$$f_2^{\pi^0}(N_{\rm ch})=CN_{\rm ch}+D \tag{14}$$

with

$$C=0.117\pm0.024 \text{ and } D=1.93\pm0.23 .$$

We note that $f_2^{\pi^0}(2)$ is consistent with zero. We can apply Eq. (14) to the two- and four-prong data by assuming $f_{2D}^{\pi^0}$ is zero for both the two- and four-prong events and using Eqs. (11) and (12). The results are

$$\alpha(2 \text{ prongs})=0.93\pm0.10 ,$$

$$\alpha(4 \text{ prongs})=0.50\pm0.13 ,$$

$$f_{1D}^{\pi^0}(2 \text{ prongs})=2.10\pm0.29 ,$$

$$f_{1D}^{\pi^0}(4 \text{ prongs})=0.92\pm0.46 .$$

The diffractive fractions α are similar to those obtained in a 205-GeV/c π^-p experiment.[10] The four-prong π^0 distributions for the diffractive and nondiffractive components, as well as for the total π^0 multiplicity, are shown in Fig. 7.

The semi-inclusive π^0 multiplicity cross sections for 2—14 charged prongs are presented in the Table IV. We

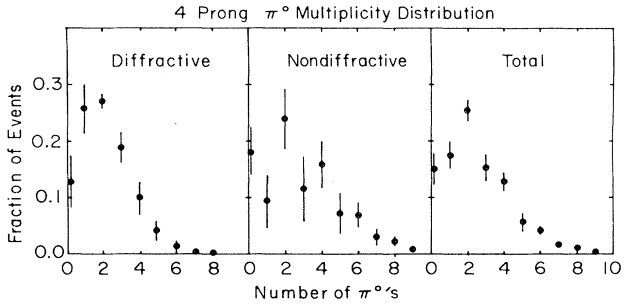

FIG. 7. The normalized diffractive, nondiffractive, and combined four-prong π^0 multiplicity distribution. The relative amounts of the diffractive and nondiffractive component are approximately equal for the four-prong events as explained in the text.

can combine these results to give the total inelastic multiplicity which is displayed in Fig. 8. The oscillatory nature of the multiplicity distribution, which peaks at even multiplicities, is at first surprising. However, this is the behavior one would expect if there were a sizable pion diffractive or other G-parity-conserving process involved. The nondiffractive component should lead to a smooth pion multiplicity distribution while the diffractive process should contribute to even multiplicities. Furthermore, the effect appears to diminish at the higher multiplicities where the diffractive component should be negligible. This oscillatory behavior of the total multiplicity distribution is also the behavior which would be expected if pions were produced in $I=0$ pairs. We have previously published[4] results based on the charged multiplicity distributions which are compatible with this production scheme. Recent results of Band *et al.*[11] also support the production of $I=0$ pion pairs at 200 GeV/c.

A caveat must be attached to Fig. 8. The error bars are purely statistical. The systematic errors which result from the assumptions previously described are undoubtedly large and difficult to estimate. Nevertheless, by drawing a smooth curve through the troughs in the distribution, we find that the total even-multiplicity excess amounts to ~4 mb. This compares with reported total diffractive cross sections for π^-p at 200 GeV/c of 3.4±0.2 mb (~1.9 mb for pion diffraction alone[10]), and 3.8±0.3 mb (2.8±0.3 mb for pion diffraction[12]). At 147 GeV/c the total diffractive cross section is 4.3 mb.[13]

ACKNOWLEDGMENTS

We would like to acknowledge the help we received from the Fermilab bubble-chamber group, especially F. R. Huson, J. P. Berge, D. Bogert, R. Hanft, R. Harris, S. Kahn, and W. Smart, during the early stages of the experiment. The scanning and measuring crews at Fermilab and Florida State are acknowledged for their work with difficult film. This work was supported in part by the U. S. Department of Energy.

APPENDIX

Let P_n be the probability that n particles are produced in an interaction. The frequency-generating function

TABLE IV. Semi-inclusive π^0 multiplicity cross sections in mb. The cross sections which appear beside the charged topology "all" are those obtained by fitting the inclusive γ-ray multiplicity distributions. It is not the sum of the π^0 cross sections for each charged topology. This sum is shown as the topology "sum."

Charged topology	Number of π^0s 0	1	2	3	4	5	6	7	8	9
2 inelastic	0.22±0.04	0.39±0.04	0.36±0.02	0.23±0.02	0.12±0.03	0.05±0.02	0.02±0.01	0.005±0.005	0.002±0.002	0 ±0.001
4[a]	0.50±0.08	0.58±0.08	0.85±0.08	0.51±0.08	0.43±0.006	0.19±0.05	0.14±0.02	0.06 ±0.02	0.04 ±0.01	0 ±0.004
6	0.63±0.11	0.29±0.20	0.93±0.22	0.40±0.28	0.68±0.24	0.29±0.21	0.34±0.17	0.13 ±0.11	0.12 ±0.09	0.05±0.05
8	0.45±0.09	0.30±0.13	0.80±0.14	0.49±0.19	0.70±0.14	0.39±0.13	0.40±0.10	0.21 ±0.07	0.17 ±0.06	0.09±0.03
10	0.18±0.04	0.31±0.03	0.48±0.03	0.52±0.05	0.52±0.02	0.43±0.03	0.33±0.01	0.23 ±0.01	0.15 ±0.01	0.09±0.01
12	0.14±0.04	0.15±0.05	0.33±0.06	0.29±0.09	0.36±0.07	0.25±0.06	0.17±0.04	0.13 ±0.04	0.13 ±0.04	0.08±0.02
14	0.06±0.03	0.08±0.03	0.17±0.05	0.18±0.06	0.21±0.05	0.18±0.06	0.16±0.05	0.12 ±0.04	0.09 ±0.03	0.06±0.02
All	1.87±0.44	3.61±0.55	3.35±0.50	3.06±0.45	2.92±0.32	2.20±0.34	1.52±0.26	1.110±0.25	0.71 ±0.26	0.43±0.24
Sum	2.18±0.18	2.10±0.27	3.92±0.29	2.62±0.37	3.02±0.29	1.78±0.27	1.56±0.21	0.93 ±0.14	0.71 ±0.12	0.38±0.07

[a]Assumes no particle correlations in diffractive component and linear equation of $f_{1N}^{\pi^0}$ and $f_{2N}^{\pi^0}$.

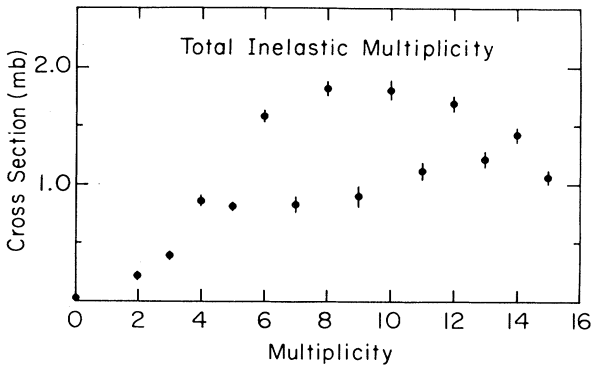

FIG. 8. The total inelastic multiplicity. The enhancement for even multiplicities is ascribed to a pion diffractive (G-parity-conserving) process. The error bars represent only the statistical errors. Systematic errors resulting from the assumptions made in the text may be large.

(FGF) for the frequency function given by $\{P_n\}$ is defined as

$$\Phi(r)=\sum_{n=0}^{\infty} P_n r^n , \tag{A1}$$

where r is a dummy variable called the generator. We can obtain P_n by differentiation,

$$P_n=\frac{1}{n!}\left[\frac{\partial}{\partial r}\right]^n \Phi(r)\Big|_{r=0} , \tag{A2}$$

and the qth factorial (binomial) moment by

$$m_{[q]}=\left[\frac{\partial}{\partial r}\right]^q \Phi(r+1)\Big|_{r=0} . \tag{A3}$$

The algebraic moments of a distribution are generated by the moment-generating function (MGF)

$$M(r)=\Phi(e^r)$$

with

$$M_q=\left[\frac{\partial}{\partial r}\right]^q M(r)\Big|_{r=0} \tag{A4}$$

being the qth algebraic moment. The generating functions

$$\Psi(r)=\ln\Phi(r+1) \tag{A5}$$

generate a set of moments called factorial cumulants, or in particle physics the Mueller moments[9]

$$f_n=\left[\frac{\partial}{\partial r}\right]^n \psi(r)\Big|_{r=0} . \tag{A6}$$

The normalized partial cross section σ_n for producing n particles of a given type is

$$\sigma_n=\frac{1}{n!}\left[\frac{\partial}{\partial r}\right]^n \exp\sum_{i=1}^{\infty} f_i \frac{(r-1)^i}{i!}\Big|_{r=0} . \tag{A7}$$

If two types of particles are produced, then Eq. (A1) can be generalized to

$$\Phi(r,s)=\sum_{i,j=0}^{\infty} P_{ij} r^i s^j , \tag{A8}$$

where r and s are now the generators for the two types of particles; the generalization of Eq. (A1) through (A6) for many types of particles being produced is straightforward.

If $\Phi(r,s)$ is a two-type FGF then one of the particle types (e.g., the one with generator s) can be ignored by setting its generator to one (e.g., $s=1$). For example, if r is the generator for charged pions and s the generator for neutral pions then

$$\Phi_{\rm ch}(r)=\Phi(r,1) , \tag{A9}$$

where $\Phi_{\rm ch}(r)$ is the charged-pion FGF and $\Phi(r,s)$ is the FGF for both neutral and charged pions.

Similarly, to ignore the difference between two types we set their corresponding generators to be equal. Thus, the FGF for pions (irrespective of charge) is given by

$$\Phi_{\pi}(r)=\Phi(r,r) . \tag{A10}$$

If a particle type with generator r decays, then

$$r \rightarrow \sum_i b_i r^{\alpha_i} s^{\beta_i} \cdots z^{\eta_i} , \tag{A11}$$

where b_i is the probability (branching fraction) of the ith decay mode, where the ith decay mode consists of α_i particles of type r, β_i particles of type s, etc.

---

*Present address: Physics Department, Notre Dame University, Notre Dame, IN 46556.

†Present address: Logicon, Inc., San Pedro, CA 90733.

[1]For a review see J. Whitmore, Phys. Rep. 27, 187 (1976).

[2]E. L. Berger *et al.*, Phys. Rev. D 7, 1412 (1973); G. H. Thomas, *ibid.* 8, 3042 (1973); A. H. Mueller, *ibid.* 4, 150 (1971); O. Czyewski and K. Rybicki, Nucl. Phys. B47, 633 (1973); D. Horn and A. Schwimmer, *ibid.* B52, 627 (1973); D. Drijard and S. Pokorski, Phys. Lett. 43B, 509 (1973); P. Grassberger and H. I. Miettinen, Nucl. Phys. B82, 26 (1974).

[3]H. Harari, in *Phenomenology of Particles at High Energies,* Proceedings of the Fourteenth Scottish Universities Summer School in Physics, Edinburgh, 1973, edited by P. L. Crawford and R. Jennings (Academic, New York, 1974), p. 247.

[4]For our two-component analysis of the charged-particle multiplicity distributions see P. Hays *et al.*, Phys. Rev. D 23, 20 (1981).

[5]D. Bogert *et al.*, Phys. Rev. D 16, 2098 (1977).

[6]R. N. Diamond *et al.*, Phys. Rev. D 25, 41 (1982).

[7]A. Fridman, Serie des Curs et Conference sur la Physique des Hautes Energies, Institut National de Physique Nucleaire et de Physique des Particules et Universite Louis Pasteur, Strasbourg, 1976, No. 11.

[8]M. G. Kendall and A. Stuart, *The Advanced Theory of Statistics* (Hafner, New York, 1963), Vol. 1.

[9]A. H. Mueller, Phys. Rev. D 4, 150 (1971).

[10]J. Lamsa *et al.*, Phys. Rev. D 18, 3933 (1978).

[11]H. R. Band *et al.*, Phys. Rev. D 26, 1013 (1982).

[12]W. D. Shephard, in *Proceedings of the Xth International Symposium on Multiparticle Dynamics, Goa, India, 1979,* edited by S. N. Ganguli, P. K. Malhotra, and A. Subramanian (Tata Institute, Bombay, 1980), p. 107.

[13]D. Brick *et al.*, Phys. Rev. D 21, 1726 (1980).